Design and qualification of a winglet with a high speed oscillating active control surface for aeroelastic wind tunnel experiments under cryogenic conditions

C. Buxel · A. Dafnis · H.-G. Reimerdes

Abstract Within the frame of the **A**ero-**S**tructural **D**ynamics **M**ethods for **A**irplane **D**esign (ASDMAD) transfer project wind tunnel experiments are carried out employing a flexible semi-span wing model. The wing model is retrofit with two different winglets, in order to investigate the unsteady aero-structural interaction. The wing model is actively excited in its modal shapes using piezoelectric actuators located in the wing root. The experiments are performed at Reynolds and Mach Numbers typical for large passenger aircraft in cruise flight at the European Transonic Windtunnel (ETW). The first configuration is a rigid, conventional winglet, while the second one is equipped with a trailing edge control surface. This control surface can be quasi-statically deflected, as well as excited at high frequency using in-situ piezoelectric actuators. This simultaneously aims at local aerodynamic trimming and active excitation or suppression of modal responses. The final design of the in-situ Active Control Surface (ACS) is a compromise between contradicting demands including the temperature range (cryogenic to room temperature), limited available space, necessary power output, strength and stiffness. Further contribution factors include implemented instrumentation, feasibility and control equipment. This paper presents on the development of this winglet in detail, including design, sizing, manufacturing and qualification.

Keywords aeroelasticity · winglet · semispan wing model · cryogenic wind tunnel experiments · active control surface

C. Buxel · A. Dafnis · H.-G. Reimerdes
Chair and Institute of Aerospace and Lightweight Structures
Wüllnerstraße 7 52064 Aachen
Tel.: +49-241-8096840
Fax: +49-241-8092230
E-mail: buxel@ilb.rwth-aachen.de

1 Introduction

The transfer project ASDMAD (**A**ero-**S**tructural **D**ynamics **M**ethods for **A**irplane **D**esign) is a cooperation between Airbus Operations GmbH and RWTH Aachen. Both partners fund this transfer project in equal shares, with Deutsche Forschungsgemeinschaft (German Research Foundation, DFG) funding RWTH Aachens share. The ASDMAD project succeeds the HIRENASD (**HI**gh **RE**ynolds **N**umber **A**ero-**S**tructural **D**ynamics) research project conducted within the framework of the collaborative research center 401 (Flow Modulation and Fluid-Structure Interaction at Airplane Wings) and completely by DFG [2].
During the HIRENASD project RWTH Aachen designed, constructed and manufactured a flexible, actively excited semispan wing model for steady and unsteady experiments in the European Transonic Wind Tunnel (ETW) in Cologne [3]. These experiments focus on aero-structural dynamic investigations under flow conditions typical for large passenger aircraft in cruise flight [4]. To obtain this at the model scale of 1:28 temperatures down to 120K and high pressure up to 4.5 bar are necessary. In order to simultaneously acquire both aerodynamic and structural information a comprehensive instrumentation is implemented.

2 Research field of the transfer project ASDMAD

The transfer project ASDMAD experimentally investigates the impact of winglets on the steady and unsteady aero-structural interaction of a flexible, semispan wing model in a transonic flow. For this purpose the HIRENASD wing model is retrofit with two different wing tip devices. The first conventional winglet

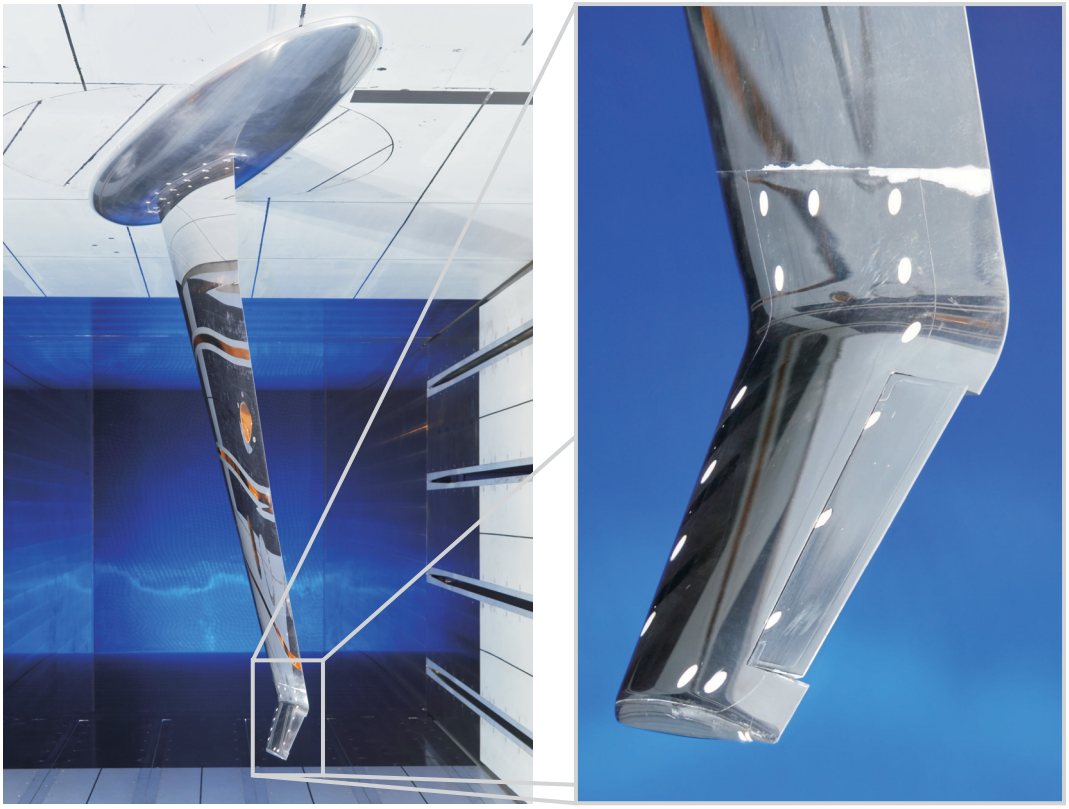

Fig. 1 Wing model with active control surface in wind tunnel

Series	Status Control Surface	Temperature [K]	Reynolds Number	Load q/E	Mach Number
1a	Active	283K	$7.1 \cdot 10^6$	$0.22 \cdot 10^{-6}$	0.75 - 0.85
1b	"	120K	$23.5 \cdot 10^6$	$0.22 \cdot 10^{-6}$	0.80 - 0.92
2a	Locked 0°	120K	"	$0.22 \cdot 10^{-6}$	"
2b	"	160K	"	$0.34 \cdot 10^{-6}$	"
3a	Locked −5°	120K	"	$0.22 \cdot 10^{-6}$	"
3b	"	160K	"	$0.34 \cdot 10^{-6}$	"
3c	"	205K	"	$0.48 \cdot 10^{-6}$	"

Table 1 Test program at ETW. Each Series included instationary experiments with active excitation (wing root and/or ACS) and stationary experiments ($\alpha_{geo} = -2°\text{to} + 6°$).

is designed to improve the overall aerodynamic performance, reducing wave drag and avoiding local flow separations with respect to load limitations of the wing model [7]. The second winglet employs an Active Control Surface (ACS) at the trailing edge of the winglet; investigating both trimming possibilities under steady state transonic aerodynamic conditions and effects an ACS excited at high frequency have on the wing models mode shapes (see figure 1). Hence, new wind tunnel testing techniques are introduced, by developing a in-situ deflection/excitation mechanism able to operate under cryogenic conditions. Besides observation and registration of aeroelastic phenomena, data for validation purposes of direct aero-structural simulation codes is amended to the HIRENASD data.

3 Description of the HIRENASD half wing model

The collaborative research center provides the elastic semispan wing model from the HIRENASD Project. Within this project the wing is designed, constructed, qualified and tested in ETW [1,3,8,9]. The basic configuration shows figure 2. The SFB 401 reference configuration with 34° leading edge sweep and 3 sections, which is typical for large transonic transport aircraft,

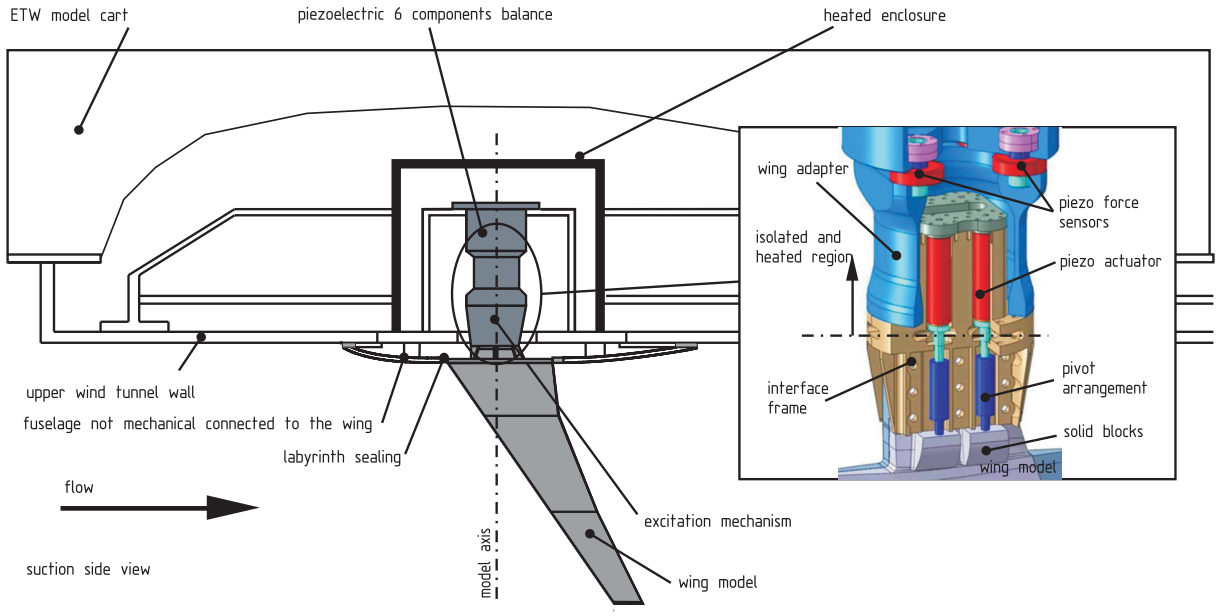

Fig. 3 Overview of test setup at ETW and detailed view of 6 components piezoelectric balance and wing root excitation mechanism

is applied at a scale of 1:28 to this wing. This leads to a semispan of 1293.93 mm with 344 mm mean chord. The BAC 3-11/RES/30/21 [10] airfoil has a 11% thickness to chord ratio which increases linearly at the inner section to 15% at the wing root.

The wing model is designed to allow large deformation resulting in noticeable fluid-structure interaction effects with low and well separated mode shapes to obtain weak modal coupling [9]. The whole test set up is mounted at the ETW model cart (see figure 3). The main components are the piezoelectric 6-components balance, the wing root excitation mechanism [8] and the wing model with new exchangeable wingtips.

The fuselage is not mechanically connected to the wing model and only serves as barrier for the top wall boundary layer towards the wing model. A labyrinth sealing prevents cold gas from flowing into the heated enclosure. Thermal heaters attached to the excitation housing form a temperature barrier between the cryogenic flow and the heated enclosure, which is heated up to room temperature. The piezoelectric 6-components balance is specifically designed and manufactured to meet the requirements of the HIRENASD project [8]. It is extraordinary stiff to show minimum deformation under static loads and its dynamic behaviour is tailored to avoid modal coupling with the wing model. The forces are measured with a set of four 3 dimensional piezoelectric, mechanically preloaded sensors with a measuring threshold of less than 1 N (see figure 3).

The figure also shows the wing root excitation mechanism consisting of 4 piezo actuators and the corresponding pivot arrangement [9]. The whole test setup is equipped with a comprehensive instrumentation. 240 in-situ pressure transducers are arranged in six cross sections and the winglet. Furthermore, 12 internal accelerometers and 6 accelerometers glued at the excitation housing and piezoelectric balance allow the models' dynamic response to be recorded and the relevant mode shapes to be decomposed with adequate accuracy. Additionally, 20 strain gauges and 14 temperature sensors are installed.

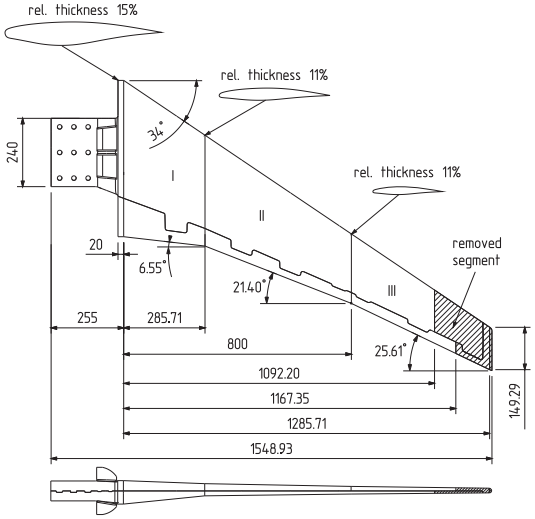

Fig. 2 HIRENASD wing model geometry with marked removed wing tip

3.1 Retrofit the HIRENASD wing model with a mechanical interface

The original HIRENASD wing model is designed to be tested only with its planar wing tip. Thus, the structure is not prepared for an exchangeable mechanical interface. As a results, within the ASDMAD project a mechanical interface configuration has to be found which holds both winglets. The design point of the mechanical interface is: Mach Number 0.80, Reynolds Number $23.5 \cdot 10^6$ and an angle of attack of 2°. Aeroelastic predictions at this point show an increase of transverse force of approx. 6% and bending moment of approx. 8% in comparision to the planar wing tip. This means three major task have to be solved: First, based on the existing structure of the wing model, an appropriate interface design has to be developed applying stress analysis and considering a smooth stiffness transition in spanwise direction from wing model to winglet. Secondly, remaining critical spots (including stress concentrations) have to be identified and attenuated by restricting aerodynamic parameters. Finally, the screwed fastening of the interface with the wing model have to be analysed and verified under the environmental conditions prevailing at ETW. The mechanical interface ultimately ranges from 85% to 91% of the semi-span of the HIRENASD wing model. Two rows of four screws each are used as fasteners. Further details are presented in [7] and figures 4 and 5 show the final interface.

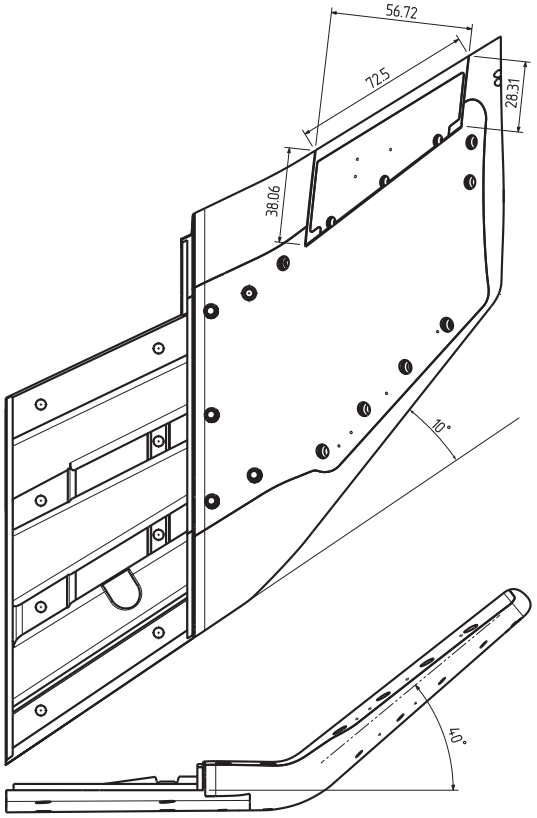

Fig. 4 Winglet outline shows 40° upward bend wingtip, 10° additional sweep and active control surface (ACS)

4 Winglet with Active Control Surface (ACS)

4.1 Geometry of the winglet and the Active Control Surface (ACS)

For the second part of the ASDMAD project the winglet with ACS outer shape was designed using CAGD techniques (Computer Aided Geometric Design) [5].
The winglets basic design feature is a 40° upward bend wingtip, which spanwidth is extended to maintain the original HIRENASD spanwidth. The leading edge sweep is enlarged from its original 34° to an additional 10° in order to improve the aerodynamic performance with respect to reduced flow separation [6]. Which is a compromise between aerodynamic performance and available space for the excitation mechanism (see figure 4). As far as necessary all aero-structural-dynamic predictions are performed with the aeroelastic software package SOFIA, developed and used by the Chair for Computational Analysis of Technical Systems (CATS), RWTH Aachen University.
The control surface shall be able to excite the wing model in its first bending mode ($25 - 30$ Hz). Aeroelastic calculations are applied to determine the required size and shape. The final control surface has a span width of 72.5 mm and a chord, linearly decreasing in wing tip direction, of 38 mm to 28.3 mm (see figure 4).

4.2 Requirements for ACS actuator mechanism

The wing model with the winglet is tested at the European Transonic Windtunnel (ETW) in Cologne. At ETW Mach number, Reynolds number and aerodynamic load factor q/E (dynamic pressure / Young's Modulus) can be varied independently. During the ASDMAD wind tunnel tests 3 configurations are tested: Series 1 with active ACS, Series 2 and 3 with locked ACS at 0° and −5° (deflected inward/upward). Each Configuration is tested at different Mach numbers and load factors while the Reynolds Number was mainly held constant at $23.5 \cdot 10^6$ (see table 1). Series 1a with a Reynolds Number of $7.1 \cdot 10^6$ was performed as first, relatively cheap test at room temperature to obtain first experience with the ACS. This included both the experimental application flow and the ACS itself.
Consequently, the ACS actuator mechanism must be

operational in a large temperature range from 110K to 300K. This fact limits the use of lubricants and standard electronic components. Furthermore, all selected materials have to be checked for temperature strain and the resulting interactions between the different components.
In order to lock the ACS at two positions a locking mechanism is required, allowing both 0° and −5° as well as a free ACS.
Finally, the design has to take into account the limited available cavity inside the wing model and the feasibility. the feasibility.

4.3 Design loads on ACS

A-priori aeroelastic simulations show, considering a ±5° deflection of the ACS, that the aerodynamic hinge moment of the ACS would reach 0.5 Nm and a resulting aerodynamic transverse force of 60 N. Although later simulations indicate a ±2° deflection of the ACS is sufficient to excite the wing model, the ±5° deflection of the ACS is applied as design parameter, in order to have a margin for unexpected effects. Inertia forces of the ACS have to be considered at an oscillation frequency of up to 30 Hz and can easily excess the aerodynamic forces and moments by a factor of four. Based on the data of prior experiments at ETW with the wing model an acceleration of 520m/s^2 is considered as contribution factor on the load estimations of the bearing of the ACS. The aerodynamic forces on the rest of the winglet were not critical and can be carried from the outer shell without inner reinforcements. This results identify as critical design features the actuator and the bearing of the control surface. From this results the actuator and the bearing are identified as the critical design features and further detail is given in the following sections.

4.4 Selection of an appropriate actuator for the ACS

The design of the actuator for the control surface is the main challenge of this project, since available space is very limited, the necessary output power is high and a great temperature span has to be covered. The loads on the ACS as described in section 4.3 along with the environmental conditions (see section 4.2) significantly influence all design decisions. The first decision concerns, in general terms, the method of converting electrical energy to mechanical energy driving the ACS. Piezoelectric actuators are an obvious choice, because they have a good energy conversion density and work, with about 30% power decay, at cryogenic temperatures. Otherwise, piezoelectric actuators are sensible to forces and moments perpendicular to their working direction (i.e. inertia forces). Another typical characteristic of piezoelectric actuators is their behaviour regarding stroke and force. Piezoelectric actuators are typically characterised through their free dutystroke and their maximum block force, but only one thing can be used at a time. For instance maximum force with no stroke or maximum dutystroke with no force. In order to gain a maximum power output piezoelectric actuators have to be used with half maximum force and half maximum stroke. To achieve this a soft spring (typically less than 5% of the piezoelectric actuators stiffness) is usually used to preload the piezoelectric actuators.

4.5 Transmitting the mechanical energy to the ACS

The piezoelectric actuators can be positioned either in the wing or in the winglet. The first alternative offers a larger available space for the piezoelectric actuators, which increases the available power in terms of force and stroke. The distance to the ACS requires a transmission able to bridge the gap between piezo actuators and ACS in the winglet. A hydraulic drive has been considered, but realizing proofed virtually impossible due to the lack of hydraulic fluids allowing the required operating temperatures. Another design applies a lever construction to convert stroke and force as required. A detailed study shows, that the elasticity of the individual components and their interfaces (e.g. pivots, contact surfaces) result in an ineffective system, which at certain conditions may not work at all.
Consequently, the whole mechanism is placed in the winglet as close to the control surface as possible, although this decision leads to a decreased available cavity. The ASDMAD winglet with ACS only offers a cuboid of 7 mm height, 50 mm width and 95 mm length. Furthermore, pivots are omitted whenever possible.
Since power generation of piezo actuators is linear dependent on its volume, as much volume as possible has to be used for the piezoelectric actuators.The cuboids available length allows a piezoelectric actuator with a free stroke of about $s_p = 100\mu$m at room temperature. At cryogenic temperatures it degrades about 30% ($df = 0.7$) and maximum power output of the actuator is reached, if operated at 50% of maximum stroke. This stroke and the corresponding force have to be converted to a combination suitable for actuating the ACS. The control surface is driven by a push/pull rod, which was clamped between both control surfaces parts. This divides the overall transmission into two parts (1. lever arm at ACS; 2. transmission from piezo

actuator to lever arm). The push/pull rod with its lever arm l_{CS} towards the axis of rotation requires a suitable combination of force and stroke. On the one hand a longer lever arm requires less force and is less sensible towards fabrication tolerances, on the other hand a larger transmission ratio from the piezo actuators to this interface is required. In short, a compromise with the longest possible lever arm considering the achievable transmission form the piezoelectric actuators has to be found. A lever arm of $l_{CS} = 2.5\,\text{mm}$ is selected and based on this configuration the required maximum input force (F) and stroke (s) can be calculated from the aerodynamic Moment ($M = 0.5\,\text{Nm}$) and the lever arm as:

$$F = \frac{M}{l_{CS}} \qquad \Rightarrow \qquad F = 200\,\text{N} \tag{1}$$

whereas the required stroke (s) is:

$$s = l_{CS} \cdot sin10^{\circ} \qquad \Rightarrow \qquad s = 0.434\,\text{mm} \tag{2}$$

So the output stroke of the transmission needs to be $s = 0.434\,\text{mm}$. This leads to a required transmission ratio (i) from the piezoelectric actuators to the push/pull rod of:

$$i = \frac{s}{0.5 \cdot s_p \cdot df} \qquad i = 12.4 \tag{3}$$

Additionally, the transmission has to fit into the cuboid and allow the piezo actuators to fill as much volume as possible to reach the necessary force, which is roughly linear dependent on the piezoelectric actuators cross section.

4.6 Applying the X-Frame as transmission

Applying the well known rules of lightweight design each element carries forces most effective, if it is loaded with push-pull forces. A concept fulfilling all these aspects is the so called X-Frame [12,11]. Additionally it only generates bearing reactions opposite of the useful forces, thus avoiding mounting difficulties. The piezoelectric actuators generate large forces, which are mainly push-pull loads onto the beams of the mechanism. Additionally, the piezoelectric actuators are supported perpendicular to their working direction and thus attenuating their vulnerability to inertia forces in that direction ,due to wing tip oscillation.
This concept is applied under the restrictions of the available space, in particular the small height and the required transmission ratio. In order to maximize the piezo volume each piezoelectric actuator has to be broad and thin and as long as possible. This ultimately leads to the configuration shown in figure 5. The available height of 7 mm is distributed as follows: 3 mm piezoelectric actuator, 2 mm connectors and isolation and 4 times 0.5 mm of mechanical components. The return spring preloads the piezoelectric actuators in order to maximize power output (see section 4.4) and serves as returning force since the X-Frame only works unidirectional.
Eventually, the temperature strain was examined and calculations show that it extend would result in an output stroke comparable to the stroke initiated by the piezoelectric actuator. Consequently, other materials with less temperature strain (e.g. INVAR®, carbon fiber reinforced plastics (CFRP)) are considered. Their properties would make the X-Frame either less effective, due to less stiffness, or much more complex to design. Subsequently, the piezoelectric actuators themselves are the solution, because at cryogenic temperatures they could be used bipolar. This possibility allowed a controlled contraction, counteracting the temperature strain. The limits of operation have to be experimentally determined (see figure 13) and finally even overcompensate the temperature strain (see section 6.3).

4.7 Bearing of the ACS

The bearing of the ACS shall be free of play, add as little friction as inevitable and carry all occurring loads (aerodynamic, inertia and excitation loads) with a mandatory safety margin of 3. As mentioned above no lubricants can be used, so the bearing has to be functional in a dry application.
The outer bearing is realized with a standard needle roller bearing, which offers a good load to space ratio, because raceways on housing and shaft are integral parts of the ACS and winglet. Although the needle roller bearing is used outside its official specifications with regard to allowed temperatures, the polyamide cage and the needles show neither defects, nor blockage, as special tests at cryogenic temperatures proof.
A set of two ball bearings serve as inner fixation of the ACS. The ball bearing is equipped with ceramic balls in order to reduce friction and allow dry operation.
The shafts on both sides of the ACS prove their safety margin applying manual calculation as well as finite element methods. Furthermore, the temperature strain between the bearing material and the surrounding Vascomax C200 steel is examined. As a results the ball bearings are ordered with a greater radial clearance to compensate the temperature strain.

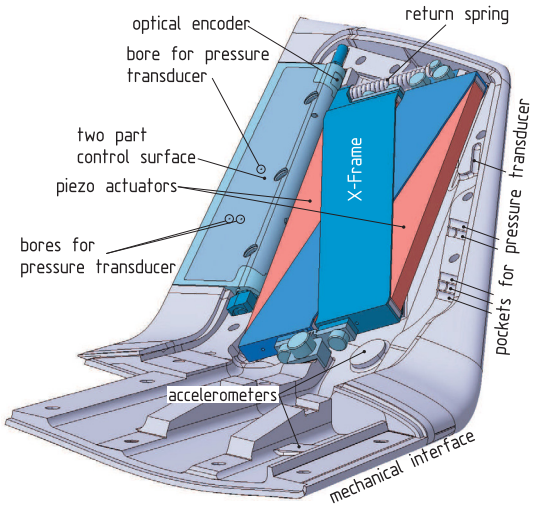

Fig. 5 Final winglet layout with X-frame and instrumentation

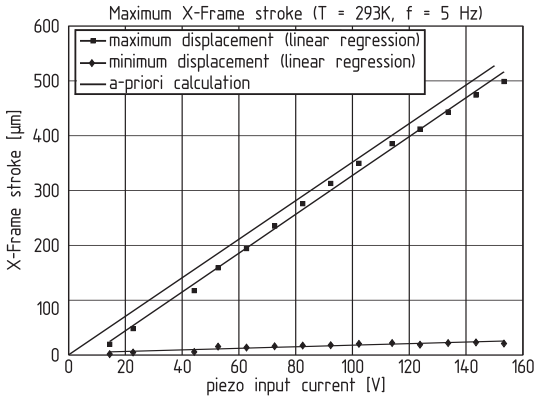

Fig. 7 Measurement of X-Frame output stroke against piezo actuator input current with linear regression and a-priori simulations with 28 elements beam model

4.8 Final design of the winglets control surface

The two piece control surface is the result of two complementary requirements. On the one hand a hollow control surface allows the integration of up to four pressure transducers (only three actually installed) and on the other hand reduces the rotational inertia of the control surface. Latter is also the reason for the fact, that the control surface is not mass balanced. Calculations with the final design of the control surface show a resulting inertia hinge moment of approx. 0.3 Nm at a $\pm 2°$ deflection angle and a 30 Hz oscillation frequency. This reduces the available moment to counter aerodynamic loads and consequently will limit the available deflection angle (see section 6.3).

4.9 Instrumentation of the winglet with ACS

Most of the winglets cavity was consumed by the actuator mechanism. Consequently, only few additional sensors could be implemented. The deflection of the ACS was detected with an in-situ, discrete optical encoder offering a resolution of approx. 0.3°, but added no friction and was fast enough to capture all occurring movements. The hollow control surface allowed the integration of three pressure transducers (two facing upward and one downward). Six further in-situ pressure transducers were implemented near the leading edge, facing both up- and downwards. In the only space left, two accelerometers were installed. Furthermore, a not shown temperature sensor was placed near the leading edge.

5 Experimental verification of the X-Frame actuator performance

After manufacturing and assembly the X-Frame is individually (i.e. without ACS) tested to assess its performance with regard to steady state and dynamic behaviour. Furthermore, the measurements are compared to the design calculations. Figure 6 shows the unrestricted stroke of the X-Frame at 5 Hz and 30 Hz and 100% voltage input. This tests allow the determination of mean minimum and maximum stroke of the X-Frame depending on input voltage and frequency. The achievable maximum and minimum stroke depending on the input voltage shows figure 7. Additionally, linear regressions and a a-priori static calculation are shown. The calculations are performed with a simple beam model consisting of 28 beam elements. Whereas the error at maximum stroke is approximately 5% (cal.: 527μm, meas.: 500μm), the gradient of both the calculation and the linear regression is almost identical ($3.51\frac{\mu m}{V}$ vs. $3.54\frac{\mu m}{V}$). Probably static friction is an important contributer to this effect, since it was not part of the simulation and both frames of the X-Frame touch each other at the center of the mechanism. This contact is inevitable due to the height restriction in the winglet. The slight increase in the achievable minimum stroke is a results of the piezo actuators hysteresis (see figure 8). This figure also shows the slight decrease of maximum stroke, if the excitation frequency is varied. Nevertheless, the frequency dependency is small as becomes clear in figure 9, so it has no effect on the utilization of the X-Frame. Therefore it can be stated, that the X-Frame design works as predicted in this configuration.

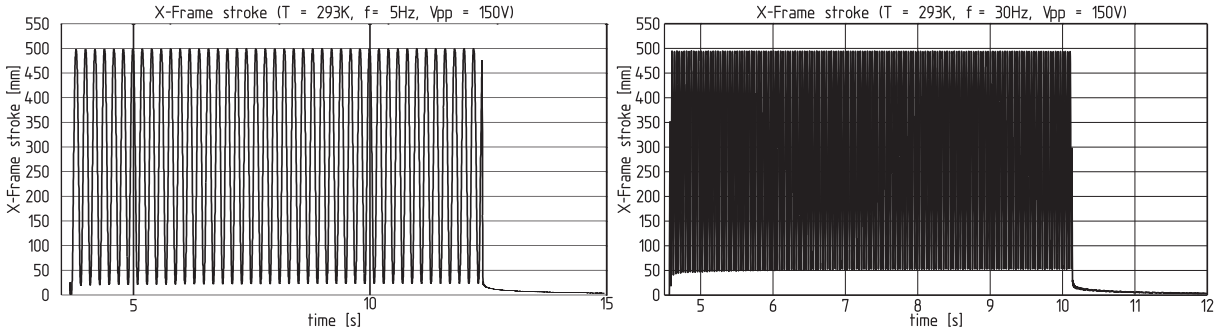

Fig. 6 Unrestricted stroke of the X-Frame at 5 Hz and 30 Hz at 100% voltage input

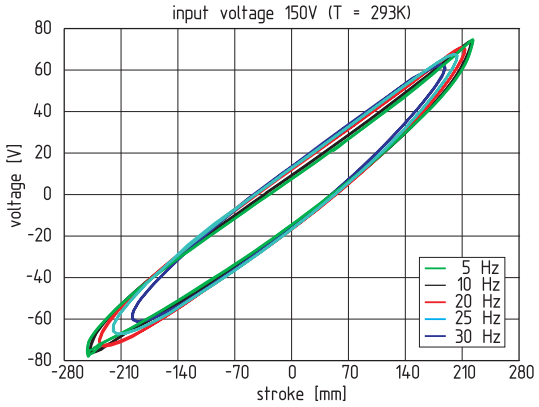

Fig. 8 Hysteresis of X-Frame with constant current amplitude and varying frequency

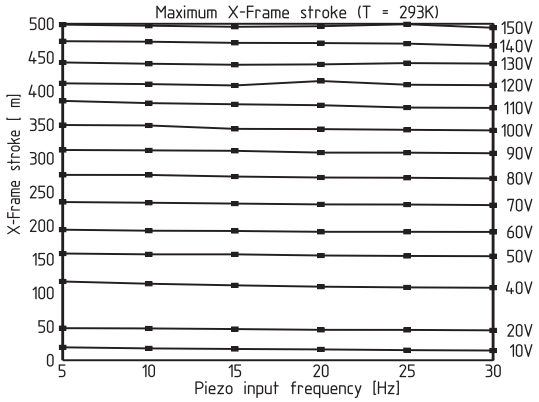

Fig. 9 Influence of frequency variation to maximum stroke of X-Frame

6 Qualification of the complete actuator system with control surface

After the initial trials the X-Frame was connected via a push/pull rod with the control surface. Further trials are performed focusing on the dynamic behaviour of the whole actuation system. Trials at Pilot European Transonic Windtunnel (PETW) include tests at cryogenic temperatures and under flow conditions comparable to ETW. PETW is a small wind tunnel with test cross section of 0.23m x 0.27m and was originally used as prototype for the much bigger ETW. The final preparation step includes a modal analysis after mounting the winglet with ACS at the wing model.

6.1 Mechanical qualification in laboratory

In order to measure the deflection of the ACS three different means of measurement are used: inclinometer, contactless measurements with a laser vibrometer and the in-situ optical encoder. The inclinometer directly delivers a deflection angle, but adds additional weight and cannot be used at high frequencies. The velocity information gained from the laser vibrometer is integrated to a displacement, but because the lever arm is not exactly known, no control surface angle can be given. The in-situ optical encoder is under development and the tests for the dynamic qualification are also used to qualify this measurement method.
Since the laser vibrometer is superior to the optical encoder in terms of resolution, both time and accuracy, only results from this sensor are shown, although both measurement techniques show the same results. Thus qualifying the in-situ optical encoder at room temperature. Further test proof, that the sensor also works reliable under cryogenic conditions, which is particular important, since it is the only available sensor to measure the control surfaces oscillation during PETW and ETW experiments.
Plug tests and free decay after active excitations with the X-Frame show a rotational eigenfrequency of the control surface of approximately $108 - 110$ Hz; varying slightly with repeated assembly.
Figures 10 and 11 show the displacement acquired with the laser vibrometer. The examination of test results with an active excitation at different frequencies and input voltage revealed, that the control surface was not

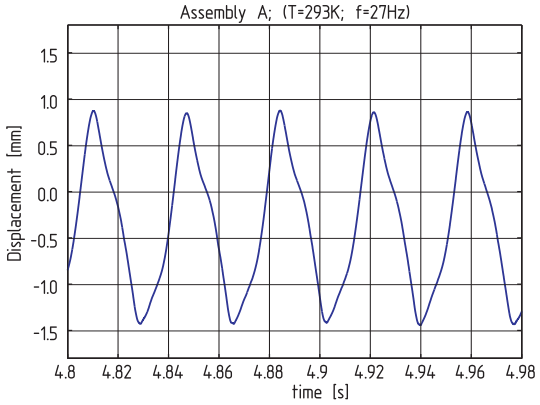

Fig. 10 Control surfaces oscillation with assembly A

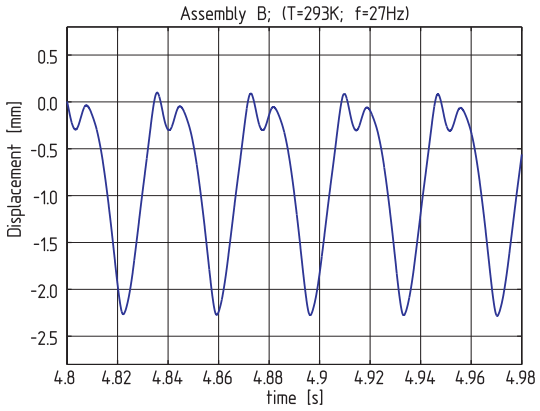

Fig. 11 Control surfaces oscillation with assembly B

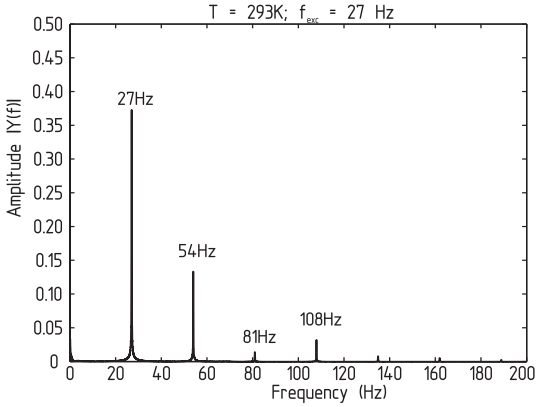

Fig. 12 FFT of oscillation assembly B clearly shows the harmonics and their interaction with the rotational frequency of the control surface

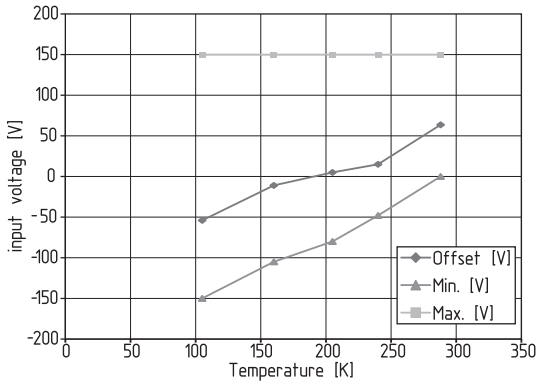

Fig. 13 Operational limits of piezoelectric actuators

always oscillating in a sinoid as expected (see figure 10 and 11). Another drawback is the fact, that slight variations during assembly (e.g. positions of bearings, tolerances of exchangeable parts) seem to have a great impact on this behaviour, as two different assemblies A and B show. Furthermore, this behaviour is dependent on the excitation frequency and had it worst behaviour around 27 Hz. This is unfortunately the projected working regime, because the control surface should influence the first bending mode of the whole wing model, which is 26.45 Hz ($T = 293$K, $M = 0.0$).
Further investigations lead to the conclusion, that the bearing evokes strong harmonics, which interact with the rotational frequency of the control surface exactly 4 times the excitation frequency (see figure 12). Due to the close schedule for test preparation this problem could not be solved. During the laboratory tests the ACS reaches frequencies of up to 40 Hz at a deflection angle of $\pm 5°$ under open loop control, which is well above the design requirements. Test at higher frequency are not conducted, in order to prevent damage to the excitation mechanism.

6.2 Temperature testing

To make sure no mechanical blockage or other abnormalities due to temperature effects occur, tests at cryogenic temperatures have to be performed. Beside the expected effect of the temperature strain, an uncommanded deflection of the ACS, no mechanical flaws are found.
During the tests at cryogenic temperatures, operation limits for the piezoelectric actuators were determined, which at low temperatures can be used bipolar (see figure 13 and section 4.6). The maximum voltage is still 150V whereas the minimun allowed voltage decreases from 0V at 293K to −150V at 120K. The Offset shows the necessary voltage to move the control surface to a 0° position. This behaviour offers two advantages, firstly the negative piezo strain compensates the temperature strain of the X-Frame and secondly the increased voltage range compensates the power decay.

mode shape	locked control surface frequency	free control surface frequency
1st flap bending	26.4 Hz	26.4 Hz
2nd flap bending	78.8 Hz	79.0 Hz
1st torsion	238.8 Hz	237.7 Hz

Table 2 Eigenfrequency of wing model with locked and free control surface

6.3 Acceptance test at PETW

The winglet with ACS had to undergo an acceptance test at PETW, in order to verify this critical component with respect to expected behaviour and possible aerodynamic phenomena, because this test was the first one with a dynamically excited control surface at ETW. Nevertheless, the aerodynamic properties were not exactly the same as in the much larger ETW, since both boundary layer and great blockage of the test section negatively influenced the flow.
The test results showed two major points, the aerodynamic and inertia moment on the control surface limits the available amplitude to about $\pm 2°$ and which is much more important, some configurations showed aerodynamic instabilities. These instabilities expressed through an oscillation of the control surface, while the rest of the winglet can be considered rigid, because of the small lever arm to the mounting point during this test. This phenomena is yet not completely understood and further research activities will be necessary.

7 Experimental survey of modal shape frequencies

The final step before entry into ETW is a modal analysis of the complete wing model assembly consisting of wing model and winglet with ACS. These tests are performed similar to previous test campaigns (HIRENASD and first part of ASDMAD) [9]. The modal parameters of the wing model are assessed applying sine sweep excitations using the wing root excitation and hammer impact method.
The modal parameters of the wing model with locked control surface are within the expected range (see table 7). The test with free control surface reveals minor interaction with the 1st flap bending and major interaction with the 2nd flap bending. The interaction can be contributed, as far as current analysis shows, to both unbalanced mass and nearness of 2nd bending and the control surfaces eigenfrequency. Further evaluations will be done in near future.

8 Conclusion

The transfer project ASDMAD investigates the impact of winglets on the steady and unsteady aero-structural interaction with a flexible, semi-span wing model in transonic flow. The wing model, reused from the HIRENASD research project, is a generic wing of a large passenger transport aircraft in a model scale of 1:28. A conventional winglet and one equipped with an Active Control Surface (ACS) are successively tested at the European Transonic Windtunnel (ETW). The second winglet is used to investigate possibilities of local aerodynamic trimming at steady state aerodynamics and active influence of excited mode shapes of the wing model. Furthermore, validation data for direct aero-structural simulation codes are generated.
Both winglets are mounted at a retrofit mechanical interface ranging from 85% to 91% of the semi-span of the HIRENASD wing model, realising a smooth spanwise stiffness transition from wing to winglet and maintain the necessary strength. The second winglet is equipped with a trailing edge Active Control Surface (ACS). The ACS is driven with an in-situ mechanism assembled of piezoelectric actuators combined with a X-Frame transmission. Beside the predescribed aerodynamic and inertia loads, the temperature range from $120-300$K, the limited space inside the winglet ($7\,\text{mm} \times 50\,\text{mm} \times 95\,\text{mm}$ cuboid), the strength and stiffness requirements, the bearing of the ACS and feasibility are the key driver of the design process.
Laboratory tests of the X-Frame mechanism without the ACS show that the maximum stroke is within 5% of the calculated values and the linearized gradient is within 1%. Due to the physical properties of the piezoelectic actuators, the mechanism shows a hysteresis as expected. This effect is frequency dependenet, but the extent is not significant up to the maximum design frequency of 30 Hz.
Further qualification tests are conducted with the ACS attached to the X-Frame. The eigenfrequency is determined with plug tests and free decay to a value of $108-110$ Hz, depending on repeated assembly. If the ACS is excited with the X-Frame the bearing evokes strong harmonics which interact with control surfaces eigenfrequency, resulting in non-sinusoidal oscillations of the ACS. This behaviour depends on repeated assembly and is not solved.
A bipolar open loop control of the piezoelectric actuators compensate the temperature strain and the temperature induced power decay. Test at Pilot European Transonic Windtunnel (PETW) proofed the readiness of the ACS for expensive ETW tests. The ACS achieved a maximum deflection angle of $\pm 2°$ during tests at cryo-

genic temperatures and high Mach Numbers.
Finally, a dynamic qualification is performed with the wing model and mounted winglet with ACS, in order to determine the eigenfrequencies. Active excitation tests, applying the wing root excitation, show a strong interaction between 2. flap bending of the wing model and control surfaces eigenfrequencies.
Nevertheless, the winglet with Active Control Surface and the wing model are qualified for the experiments, which were carried out at ETW in March 2011.
Further evaluations are going to focus on structural interaction between ACS and the semi-span wing model. Future projects will incorporate a closed-loop control to suppress the first flap-bending eigenmode.

Acknowledgements This transfer project is funded by German Research Foundation (DFG) and Airbus Operations GmbH in equal shares and is also carried out in cooperation with Airbus Operations GmbH, Germany.

References

1. J. Ballmann, C. Braun, A. Dafnis, H. Korsch, H.-G. Reimerdes, K.-H. Brakhage, and H. Olivier. Numerically predicted and first experimental results of the hirenasd projectnumerically predicted and first experimental results of the hirenasd project. In *DGLR Jahrestagung, Braunschweig*, 2006. Paper DGLR-2006-117.
2. J. Ballmann, A. Dafnis, K.-H. Brakhage, C. Braun, A. Baars, H. Korsch, C. Buxel, H.-G. Reimerdes, and H. Olivier. Transonic high reynolds number aerostructural dynamics experiments in the european transonic windtunnel. In *International Forum of Aeroelasticity and Structural Dynamics (IFASD), Stockholm*, 2007. Paper IF-061.
3. J. Ballmann, A. Dafnis, K.-H. Brakhage, C. Braun, M. Kämpchen, H. Korsch, H.-G. Reimerdes, and H. Olivier. The hirenasd elastic wing model and aeroelastic test program in the european transonic windtunnel (etw). In *DGLR Jahrestagung*, 2005. Paper DGLR-2005-264.
4. J. Ballmann, A. Dafnis, C. Braun, H. Korsch, H.-G. Reimerdes, and H. Olivier. The hirenasd-project: High reynolds number aerostructural dynamics experiments in the european transonic windtunnel (etw). In *International Council of the Aeronautical Sciences (ICAS) Congress, Hamburg*, 2006. Paper-No. 2006-5.11.2.
5. K.-H. Brakhage. Generating airplane wings for numerical simulation and manufacturing. In *9th International Conference on Numerical Grid Generation, San Jose*, 2005.
6. B.-H. Chen, K.-H. Brakhage, M. Behr, and J. Ballmann. Numerical simulations for preparing new aero-structural dynamic experiments in etw with a modified hirenasd wing model. In *International Forum of Aeroelasticity and Structural Dynamics (IFASD), Seattle*, 2009.
7. A. Dafnis, C. Buxel, J. A. Kengmogne, S. Büsing, H.-G. Reimerdes, M. Behr, B.-H. Chen, L. Reimer, A. Bouke, K.-H. Brakhage, H. Olivier, M. Kordt, F. Theurich, A. Büscher, J. Brink-Spalink, and J. Ballmann. Stationäre und instationäre untersuchungen an einem elastischen flügelmodell mit winglet im kryogenen windkanal im rahmen des asdmad-projektes. In *Deutscher Luft- und Raumfahrtkongress (DLRK), Hamburg*, 2010.
8. A. Dafnis, H. Korsch, C. Buxel, H.-G. Reimerdes, C. Braun, and J. Ballmann. Dynamic response of the hirenasd elastic wing model under wind-off and wind-on conditions. In *International Forum of Aeroelasticity and Structural Dynamics (IFASD), Stockholm*, 2007. Paper IF-073.
9. H. Korsch, A. Dafnis, H.-G. Reimerdes, C. Braun, and J. Ballmann. Dynamic qualification of the hirenasd elastic wing model. In *DGLR Jahrestagung, Braunschweig*, 2006. Paper DGLR-2006-045.
10. I. R. M. Moir. Measurement on a two-dimensional aerofoil with high-lift devices. In *AGARD-AR-303*, volume 1, pages 58–59, 1994.
11. E. F. Prechtl. *Design and Implementation of a Piezoelectric Servo-Flap Actuation System for Helicopter Rotor Individual Blade Control*. PhD thesis, Massachusetts Institute of Technology, 2000.
12. E. F. Prechtl and S. R. Hall. Design of a high efficiency, large stroke, electromechanical actuator. *Smart Materials and Structures*, 8:13–30, 1999.